GEOQuébec 2015
Challenges from North to South
Des défis du Nord au Sud

PIERRE 2: A Stochastic Rock Fall Simulator – Development, Calibration and Applications

Andrew Mitchell & Oldrich Hungr
Department of Earth, Ocean and Atmospheric Sciences – University of British Columbia, Vancouver, BC, Canada

ABSTRACT
Computer models have become standard in assessing the hazards posed by rock falls, with a wide variety of models currently available. The PIERRE 2 model, presented here, returns to a simplified lumped-mass model assuming collinear impact conditions. The natural variability of rock falls is represented using:

- A stochastic roughness angle applied to the slope;
- Hyperbolic restitution factors to define the conservation of momentum; and,
- A stochastic shape factor, used to vary the sphere dimensions at impact.

Impact mechanics theory was used as the basis for these features. Their validity is demonstrated through extensive 2D and 3D model calibration for five distinct sites. The calibration was directed to optimal simulation of rock fall behaviour in multiple dimensions, including runout distance, jump height and both linear and rotational velocity. The focus of the model development was to produce accurate statistical distributions of the outputs for hazard assessments with limited site information.

RÉSUMÉ
La chute des roches est un aléa qui est évalué en général avec des logiciels numériques, et il existe une variété de logiciels disponibles. Le logiciel PIERRE 2, présenté ici, utilise le modèle de masse concentrée, supposant des conditions d'impact colinéaire. La variabilité naturelle est représentée avec :

- La rugosité stochastique appliquée à la pente;
- Les facteurs de restitution hyperbolique définissant la conservation d'élan; et,
- Un facteur de forme stochastique, utilisé pour faire varier la dimension de la sphère à l'impact.

La théorie de la mécanique d'impact a été utilisée pour les fondements du logiciel. La validité est démontrée avec le calibrage extensif pour les modèles 2D et 3D du logiciel pour cinq sites distincts. L'objectif du calibrage fut la simulation du comportement des roches, y compris le point d'arrêt, la hauteur de passage, la vitesse linéaire et la rotation. L'objectif du développement du logiciel était de faire une distribution statistique précise du rendement pour la détermination des aléas avec des informations restreintes sur le site.

1 INTRODUCTION

Rock falls are a common hazard affecting people and infrastructure below natural cliffs and in man-made environments such as roads, railways, quarries and open pit mines. The total volume of material in these events is often limited, but the rock fragments will usually attain extremely rapid velocities, thus the affected areas are relatively small, but the intensity of the impact is high (Volkwein et al., 2011). The potential source areas are also typically widely distributed.

Computer models have become standard in assessing the hazards posed by rock falls, and there are a wide variety of models currently available. The main difference between these models is in how they represent the impact process. New models utilizing rigorous solutions for rigid body impacts have become more common; however, the complexity of these models makes them difficult to calibrate and difficult to apply in practice. Because the source areas are widely distributed, simpler rock fall models designed for large-scale hazard mapping have become more popular, but these models tend to use extremely simplified impact representations. The work here details a model that uses a simplified impact representation so that it can be effectively applied over large areas, but the simplifications are based on impact mechanics theory in order to produce more realistic results.

The PIERRE 2 stochastic rock fall simulation program is presented in its 2D and 3D versions. An extensive calibration and validation program showed that the model can reproduce runout and kinematic behaviour of rocks based on relatively limited site characterization data. The use of the model outputs as the inputs for probabilistic rock fall protection system design and quantitative hazard assessment is also described.

2 MODEL DESCRIPTION

The PIERRE 2 model has been developed using a simplified impact representation, assuming the rocks can be approximated as spheres, undergoing collinear impacts on planar surfaces. Fragmentation is not considered in the present version of the model, thus the mass of the particle is constant throughout the trajectory. To create the naturally observed variability in rock fall trajectories, a stochastic variation of the slope angle at the impact site is introduced to replicate the net effects of the irregularity of both the natural boulder shapes and the slope surface. The conservation of momentum during impacts is described using hyperbolic restitution factors that vary depending on impact conditions. The diameter of the assumed sphere is also stochastically varied at impact to better represent the rotational-translational partitioning of energy.

Between impacts, the model represents the flight phase of the trajectories using the classic ballistic parabola. Frictional sliding motion is also considered in the model. This model has been developed in parallel in 2D and 3D versions.

2.1 Roughness Angle

The roughness angle, θ, defined here is similar to the one used in CRSP (Pfeiffer and Bowen, 1989) and other models. The difference is that our roughness angle is meant to represent the combined effects of the variability of the particle shape and the slope surfaces, and is not strictly defined in geometrical terms. At each impact, the roughness is applied to the slope surface by subtracting from the local slope angle. Negative roughness is not considered, as this could result in trajectories with the particle below the slope surface.

Trials with various distributions were attempted, with a truncated normal distribution ultimately being selected (Mitchell, 2015). The distribution used for the 2D roughness is calculated using Eq. 1, which is the Box-Muller approximation of a normal distribution with a mean and standard deviation both equal to 0.5, created by drawing two random numbers between 0 and 1, S_i and S_j. The width of the distribution is set by the user-input θ_{scale} value.

$$\tan\theta = \theta_{scale}[0.5 + 0.5\cos(2\pi S_j)(-2\ln(S_i))^{1/2}] \qquad [1]$$

The 3D model requires two roughness angles: one in the longitudinal direction, defined in the vertical plane containing the incident trajectory, and the other in the transverse direction, which is perpendicular to the longitudinal direction. The longitudinal roughness is defined in the exact same way as the 2D roughness, using Eq. 1. The transverse roughness, designated ψ, also uses a normal distribution, but a symmetrical one, with a mean of zero, and allowing negative values, as shown in Eq. 2.

$$\tan\psi = \psi_{scale}[0.5\cos(2\pi S_j)(-2\ln(S_i))^{1/2}] \qquad [2]$$

2.2 Restitution Factors

The conservation of momentum or energy during an impact is typically calculated by applying empirically derived coefficients of restitution. Looking at the various studies on this topic, there is a wide range of values reported for the same material, and different materials may have overlapping ranges, see Turner and Duffy (2012, Table 8-3) for a review. A review of relevant literature from the field of impact mechanics also shows that while the substrate properties have an effect, the impacting body's dimensions and incident velocity will also have an effect (Goldsmith, 1960, Forrestal and Luk, 1992, Pichler et al, 2005). For clarity, the term coefficient of restitution is replaced with restitution factor, in recognition of the fact that momentum conservation is not simply a property of the substrate material.

During impacts, energy is spent by deformation, fracturing, friction and mass displacement (cratering), all of which intensify with increased incident kinetic energy. To account for this, the restitution factors in the PIERRE model are scaled by a hyperbolic function, proposed by Bourrier and Hungr (2012), with the restitution factor determined by the incident momentum. The present version of the model has the restitution factors scaled to the incident "deformation energy", designated E_d, defined as the ratio of the incident kinetic energy over the contact area, having characteristic dimensions of Dv_n^2, where D is the rock equivalent diameter and v_n is the incident normal velocity. The theoretical basis of this is presented in Mitchell (2015).

Using a hyperbola, the momentum conservation for an impact can be described by a single reference point where there is 50% momentum conservation, $E_{n,50}$ and $E_{t,50}$ for the normal and tangential directions, respectively. The normal and tangential restitution factors relative to the local slope rotated by the roughness angle(s), k_n' and k_t', are shown in Eq. 3:

$$k_n' = \frac{E_{n0.5}}{E_d + E_{n0.5}} \qquad k_t' = \frac{E_{t0.5}}{E_d + E_{t0.5}} \qquad [3]$$

In the 3D version of the model, the tangential restitution factor is applied to both the longitudinal and transverse velocities.

2.3 Shape Factor

Boulders are represented as spheres in the program, with their equivalent radius determined from the mass of the boulder. The distance between the centre of mass and the impact point for an irregular shaped boulder will likely be different than the equivalent spherical radius and this has an effect on the rotation of the boulder. A shape factor that varies the radius at impact between a user defined minimum and maximum is included in the model to better represent the rotation of the boulders. (Note: this feature does not address the collinearity issue, it only improves the estimation of rotational impulse during impact.)

2.4 Impact Model

When the program detects an impact with the slope surface, it will calculate a random roughness angle. The restitution factors are then calculated relative to the local slope modified by the roughness. Finally, a random shape factor is calculated, and the resulting quantities are used in the calculations for momentum conservation.

The equations derived by Goldsmith (1960) for the impact of a rigid sphere on an infinitely massive planar surface have been used as the basis for this impact model. The first stage is to calculate the inclination of the incident impulse vector, called the friction limit angle, γ:

$$\tan\gamma = \frac{2\left(k_{t'} v_{t'}^{in} + R_{eff} k_{t'} \omega^{in}\right)}{7 v_{n'}^{in}(1 + k_{n'})} \qquad [4]$$

During an impact, slip will occur, which is sliding motion at the contact point. If the slip is fully contained within the impact period, the rotational and tangential velocities will be synchronized, i.e. $v_t^{re} = R\omega^{re}$. This scenario occurs when the interface friction angle, ϕ, is greater than γ. In this case, termed a contained slip impact, the following equations are used:

$$\begin{vmatrix} v_{t'}^{re} \\ v_{n'}^{re} \\ R\omega^{re} \end{vmatrix} = \begin{vmatrix} \frac{5}{7}k_{t'} & 0 & -\frac{2}{7}k_{t'} \\ 0 & -k_{n'} & 0 \\ -\frac{5}{7}k_{t'} & 0 & \frac{2}{7}k_{t'} \end{vmatrix} \times \begin{vmatrix} v_{t'}^{in} \\ v_{n'}^{in} \\ R_{eff}\,\omega^{in} \end{vmatrix} \qquad [5]$$

If synchronization of the rotational and tangential velocities has not occurred during the impact, the situation is termed an uncontained slip impact, and the following set of equations are used:

$$\begin{vmatrix} v_{t'}^{re} \\ v_{n'}^{re} \\ R\omega^{re} \end{vmatrix} = \begin{vmatrix} k_{t'} & -\tan\varphi\,(1 + k_{n'}) & 0 \\ 0 & -k_{n'} & 0 \\ 0 & -\frac{5}{2}\tan\varphi(1 + k_{n'}) & k_{t'} \end{vmatrix} \times \begin{vmatrix} v_{t'}^{in} \\ v_{n'}^{in} \\ R_{eff}\omega^{in} \end{vmatrix} [6]$$

This impact calculation is also used in the 3D model, with the tangential restitution factor applied to the longitudinal and transverse linear and rotational velocity components. Further details on the 3D model are presented in Gischig et al. (2015).

Within this relatively simple framework, the stochastic roughness, variable restitution factors and stochastic shape factor (parameters listed in Table 1) are able to represent the naturally observed variation in trajectories. The validity of the model is demonstrated by the calibration process, detailed in the following section.

3 2D CALIBRATION & VALIDATION

The model was calibrated using data from experiments with detailed kinematic information on two natural slopes, Vaujany, France and Ehime, Japan, and excavated slopes at three Austrian quarries. The results from the calibrations were then applied to a natural slope, Tornado Mountain, and an excavated slope at Nicolum quarry, both in British Columbia. The model parameters have been determined by calibration, either through systematic parametric or Monte Carlo simulations, or by trial and error. Despite having a relation to physical properties of the materials, the parameters are not strictly physically based. Details of the specific calibrations to determine values for the model inputs are given in this section.

The Vaujany test site is located on a talus slope with an avalanche channel that is free of large trees on the upper slope section. A forest road crosses the test slope approximately 150 vertical m lower than the release point, and below that is a more conical slope consisting of coarser talus. In 2003 experiments carried out by IRSTEA, Grenoble, a total of 100 rocks were released and the runout distances were recorded along with the jump heights and velocities at two locations on the upper slope, designated Screen 1 and Screen 2. Further details of the site and the experimental program are provided in Dorren et al. (2005).

An initial parametric study was carried out to determine the model sensitivity to the roughness and normal deformation energy, and to narrow the range of inputs for detailed calibrations. A set of inputs were found that gave a reasonable compromise between being able to predict the runout distribution and the jump height and the velocity distributions simultaneously. Details of this study will be presented in a future paper. The main conclusions from the initial parametric study were:

- The model is most sensitive to roughness;
- Increasing roughness will decrease runout, velocity and the average jump height; however, higher roughness values are necessary to produce the extreme values for jump height; and,
- Increasing the normal deformation energy will increase runout and jump height.

Following the initial calibration with the Vaujany data, these same parameters were applied to the Ehime simulation. The Ehime test site is an open slope approximately 45 m high, with weak bedrock thinly mantled with soil transitioning to a compact talus slope. These tests included information on both linear and rotational velocities, which allowed for the calibration of the shape factor. The tests used four cast concrete spheres and seven cast cubes, as well as 12 natural rocks. The calibrated parameters from Vaujany provided good estimates of the linear velocities (Figure 1), but tended to over-predict the rotational velocity. To address this, plots provided by Ushiro et al. (2006) showing the relationship between the rotational and linear kinetic energy were used to calibrate the shape factor.

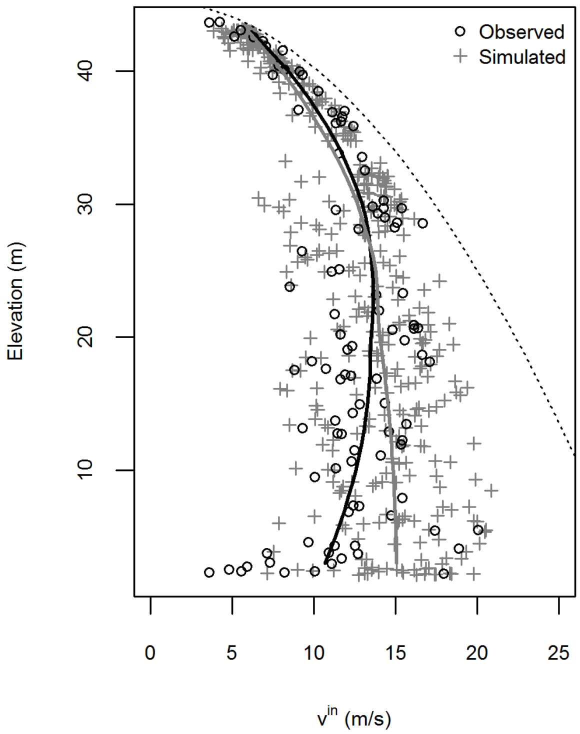

Figure 1. Incident velocity, v^{in}, vs. elevation plot for the Ehime natural rock simulation.

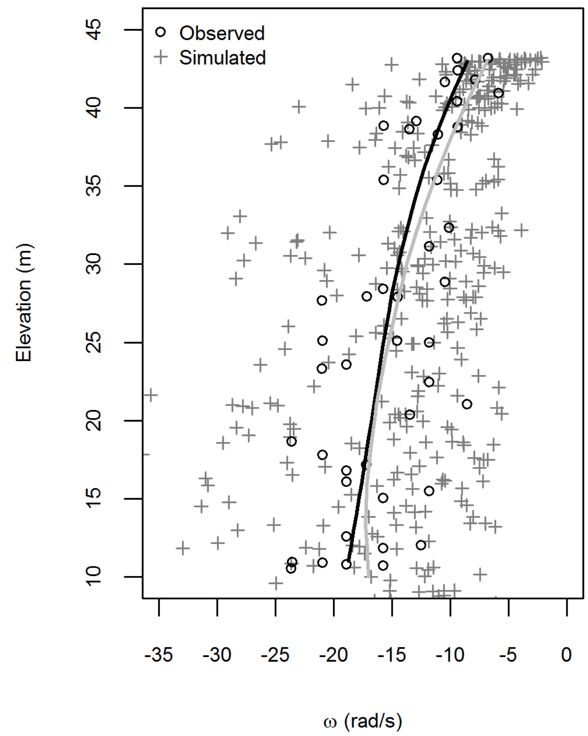

Figure 2. Rotational velocity vs. elevation plot for the Ehime natural rock simulation.

By including the shape factor, it was possible to more closely reproduce the observed relationships between the rotational and linear kinetic energy. By doing this, the prediction of the rotational velocity, ω, is also improved, as shown in Figure 2, and the prediction of the linear velocity is not strongly affected. The range of rotational velocities predicted by the program is still greater than what was observed, but the inclusion of the shape factor improves the overall prediction for rotational velocity.

The Vaujany model was re-run with the shape factor for a final calibration. The results for the runout distribution, shown in Figure 3, and jump height and velocity distributions, Figure 4, all matched well at this final stage. The calibrated parameters are listed in Table 1.

Table 1. Summary of Vaujany/Ehime calibrated model inputs.

Model Input	Firm Talus	Forest Road
θ_{scale}	0.7	0.4
$E_{n,50}$	15	
$E_{t,50}$	50	
φ	30°	
Shape (min – max)	1.0 – 1.5	

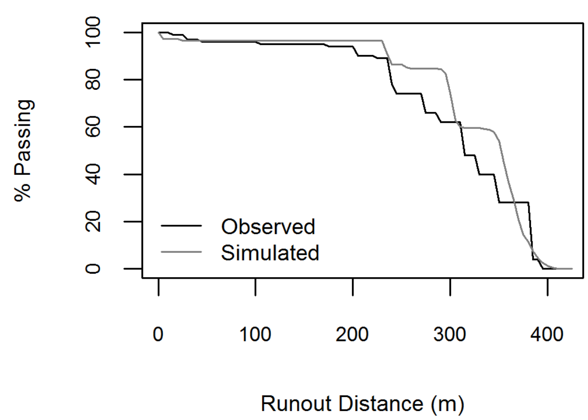

Figure 3. Observed vs. simulated runout distributions for the Vaujany calibrated model.

These parameters calibrated from Vaujany and Ehime were applied directly to the Tornado Mountain model in a pseudo-forward analysis. A detailed description of the site is provided by Wyllie (2014). At this site in eastern British Columbia, two large boulders detached from a cliff and travelled over 600 m down a talus slope, breaking small trees on their way. The tree-strike locations were taken as an indication of the jump height for comparison. Each boulder was simulated with 50 trajectories. The jump height and final stopping positions were reasonably predicted by the model results, shown in Figure 5.

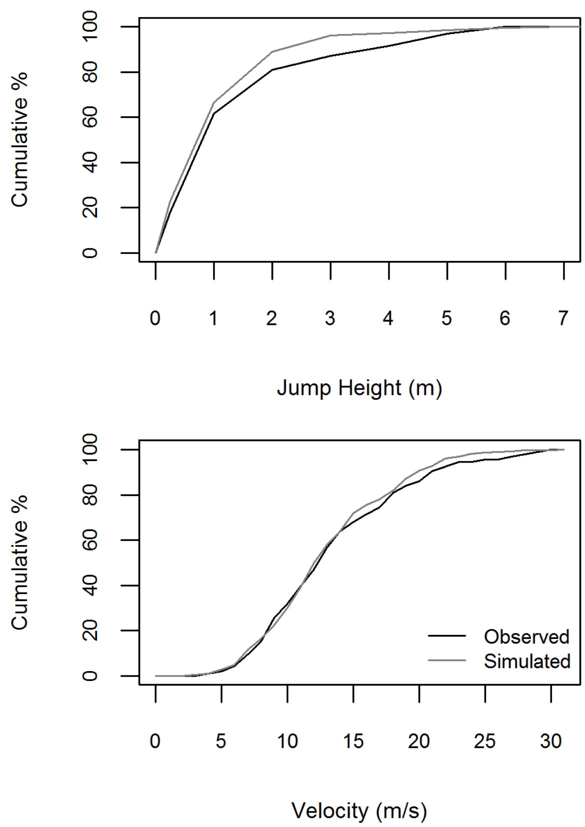

Figure 4. Observed vs simulated jump height and velocity distributions at the Screen 2 location for the Vaujany calibrated model.

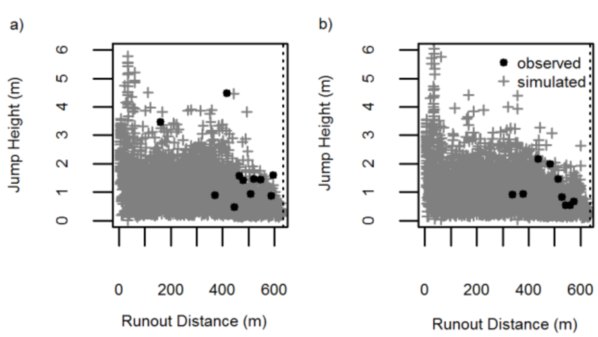

Figure 5. Observed vs simulated jump height vs. runout for boulders a and b, observed runout shown by the dashed vertical line for the Tornado mountain model.

Calibrations were also carried out for hard, exposed rock quarry slopes. The calibration data was taken from three Austrian quarries. This was done as part of a broader study on hazard zones within quarries, currently in review (Preh et al., 2015). The results of that calibration are summarized in Table 2. The shape factor was not considered in this calibration.

Table 2. Summary of Austrian quarry calibrated model inputs.

Model Input	Quarry Face	Quarry Floor
θ_{scale}	0.65	0.35
$E_{n,50}$	5	
$E_{t,50}$	50	
Φ	30°	

The effect of the input profile resolution was also tested by Preh et al. (2015). The results obtained using photogrammetry data with a resolution of approximately 3 cm, and those obtained by smoothing the profile to its general shape, with section lengths of several metres, showed very little difference. For example, the predicted 95th percentile runout distance increased between 1% and 5% using the smoothed topography for the sites tested (Preh et al. 2015).

The model parameters calibrated from the Austrian quarries were applied to the Nicolum quarry in BC. Data from experiments conducted by the Ministry of Transportation and UBC Geological Engineering in 1998 were used for comparison. During these experiments, 34 rocks were released from the top of the quarry and videotaped as they fell approximately 80 m to the quarry floor. Grid marks were painted on the quarry face and surveyed. By analysing the impact locations and timing from the videos, the trajectories could be reconstructed, allowing for the determination of the jump heights and velocities. It can be seen in Figure 6 that applying the parameters calibrated from the Austrian study to Nicolum results in a good prediction of the velocity vs. elevation.

4 3D CALIBRATION

A 3D version of this model has been developed in parallel with the 2D model. A description of the model and the results of an initial calibration have been published (Gischig et al., 2015). The 3D Vaujany model presented by Gischig et al. has been recalibrated with the new roughness angle distribution (Eq. 1 and 2), and the shape factor. The second calibration was also done with the objective of having as many of the parameters matching the 2D calibrated parameters as possible. Using the parameters given in Table 3, the runout prediction and the velocity and jump height predictions at both Screen locations matched the observations and the 2D simulation results well.

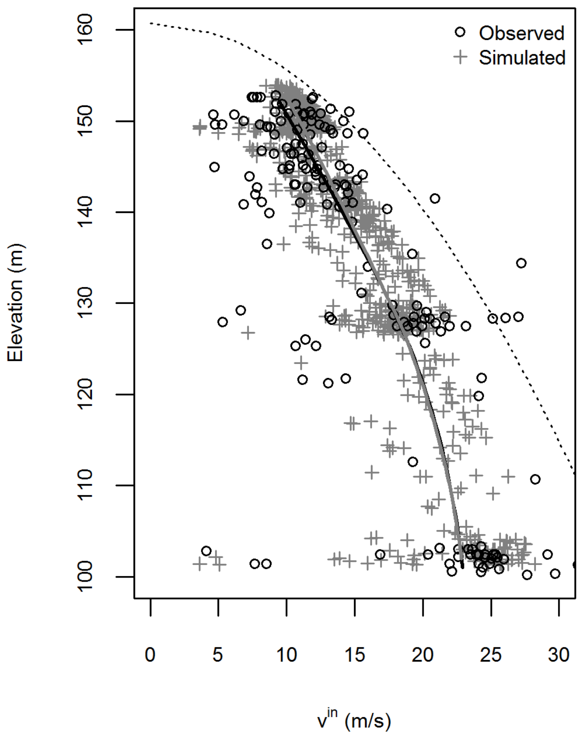

Figure 6. Incident velocity vs. elevation plot for the Nicolum simulation.

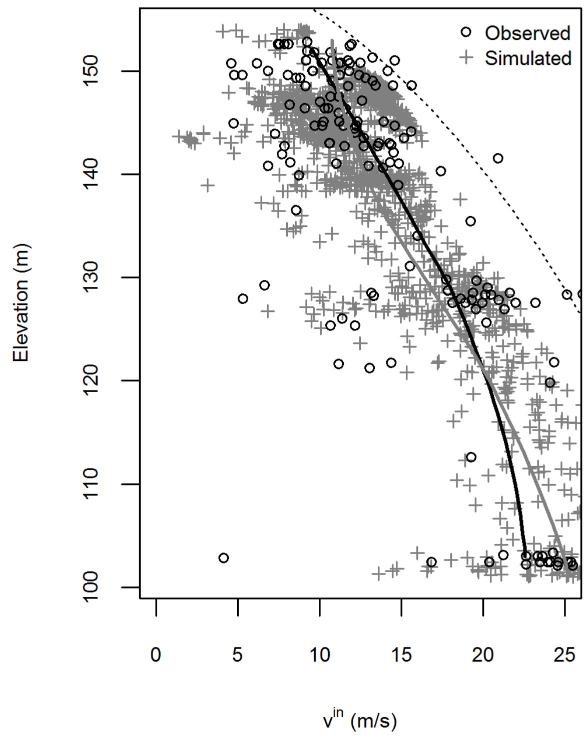

Figure 7. Observed vs. simulated velocity for the 3D Nicolum model.

Table 3. Summary of the 3D Vaujany calibrated model inputs.

Model Input	Upper Talus	Forrest Road	Lower Talus
θ_{scale}	1.0	0.4	1.5
ψ_{scale}	0.9	0.3	1.0
$E_{n,50}$	15		
$E_{t,50}$	50		
φ	30°		
Shape (min – max)	1.0 – 1.5		

A 3D version of the Nicolum quarry model was also produced. The deformation energy and friction angle parameters found in the Austrian quarry calibrations were used directly in the 3D model. The roughness angle was set so that the total roughness would be similar to the 2D model and the ratio between the longitudinal and transverse roughness would be similar to that found for the Vaujany simulation. By doing this, it was possible to approximately match the areal distribution of impacts, and the velocity versus elevation profile, shown in Figure 7.

5 APPLICATIONS

Aside from validating the model with pseudo-forward analyses from the Tornado Mountain and Nicolum datasets, the model outputs were used as design input values and compared to the observed data with reliability engineering principles for the Vaujany data. The ETAG 027 rock fall barrier design guidelines (Peila and Ronco, 2009) were used to determine interception height, h_i, serviceability energy limit (SEL), and maximum energy limit (MEL) for hypothetical barriers at the Screen 1 and Screen 2 locations using the 2D and 3D versions of the model. Using reliability engineering principles, the probability of the design parameters derived from the model being exceeded were calculated (Duncan, 2000).

Following the ETAG 027 guidelines, the 95th percentile (P95) for the jump height and for the velocity at each Screen location were calculated. The rocks used in the test were all of a similar size, thus differences in behaviour were not noted during the experiments, i.e. the jump height and velocity were independent of the rock mass for the range of sizes tested. The maximum volume recorded in the test was used in the calculation of the design block mass. Factors of safety were selected for a high confidence in the topography and block size, and trajectory information derived from computer modeling. To determine the reliability of the prediction, i.e. the probability that the factor of safety is less than 1, Weibull distributions were fit to the observed datasets so that design values outside the range of the observations could be evaluated.

The results of the hypothetical design for h_i, SEL, and MEL along with the probability of exceedance, P(E), from comparison to the Weibull distributions fit to the observed data are summarized in Table 4.

Table 4. Summary of hypothetical design values and probabilities of exceedance

Model	**Screen 1**	**h_i**	**SEL**	**MEL**
2D	Design	4.02 m	1070 kJ	1390 kJ
	P(E)	2.4 %	0.072 %	0.004 %
3D	Design	4.66 m	1020 kJ	1320 kJ
	P(E)	1.1 %	0.18 %	0.019 %
Model	**Screen 2**	**h_i**	**SEL**	**MEL**
2D	Design	4.16 m	1150 kJ	1490 kJ
	P(E)	6.2 %	0.099 %	0.006 %
3D	Design	4.91 m	1320 kJ	1610 kJ
	P(E)	3.3 %	0.002 %	5E-5 %

Examination of the P(E) values shows the minimum design barrier height obtained from the P95 simulation values achieves approximately that level of containment. Although the P95 jump height from the simulation is somewhat under-predicted, the applied factors of safety decrease the probability of failure significantly. If greater than 95% containment is desired, a higher factor of safety should be applied to the model results. The design SEL and MEL values are conservative in all cases because the predicted P95 values for the velocity were close to the observations.

Beyond determining the height and design energy, 3D simulation results can be used to determine the required width for rock fall protection systems. Using the Vaujany simulation, a map of the areas potentially impacted from a localized source, shown as the probability of impact, can be produced, with an example shown in Figure 8.

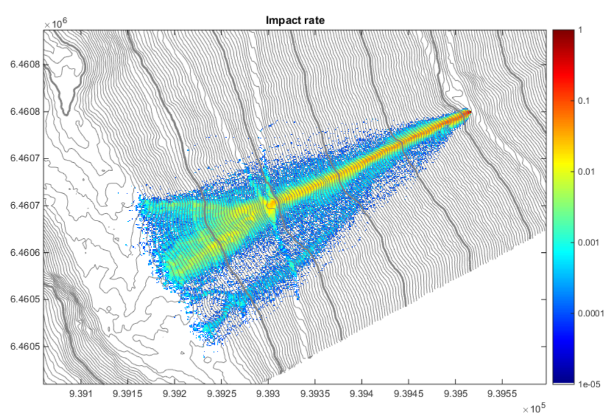

Figure 8. Impact probability map for the Vaujany simulation.

By selecting a target containment, say 99%, a barrier would have to have a width crossing all the areas with a probability of impact greater than 0.01 (the yellow zones on the impact map).

Another application is creating quantitative hazard maps. The simulation results can be used to compile maps showing the return period for trajectories exceeding a certain energy threshold (Abruzzese and Labiouse, 2014). The trajectory data can be filtered to show the frequency of boulders with a jump height or kinetic energy greater than some threshold. An example of a map prepared with a threshold kinetic energy of 500 kJ is shown in Figure 10. If we assume the site has, on average, one rock fall event of this magnitude every year (1.0 to 1.4 m equivalent diameter for the simulation), the annual probability of a boulder of that magnitude impacting an area can be determined directly from the map.

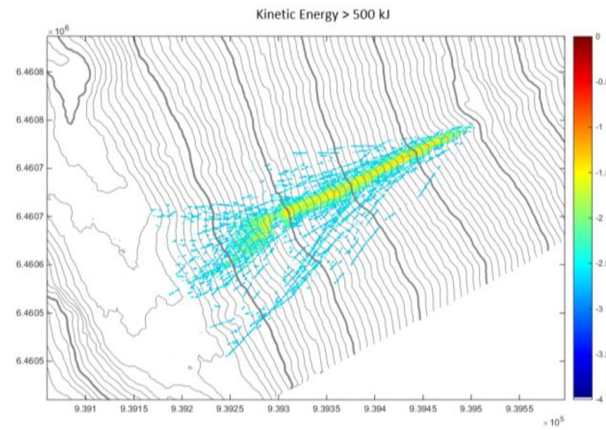

Figure 9. Probability of kinetic energy > 500 kJ map for the Vaujany simulation. Note the logarithmic scale for the probability of exceedance.

It can be seen that the total area potentially affected by rock fall impacts is quite large (Figure 9), but the area with a higher probability of a high intensity impact is much smaller, mostly confined to the well-defined channel in the upper slope.

6 CONCLUSIONS

The recent trend in computer modeling of rock falls has been towards making increasingly complex rigid body models. The model presented here has returned to a simpler, lumped mass particle representation, with stochastic elements to achieve the variability that is observed in actual rock fall events. The level of detail required for the model inputs is in line with the relatively limited site information typically available during field studies. The speed of modern processors can be utilized to create statistically significant samples of simple model runs as opposed to making fewer model runs of a more complex – and more poorly constrained – model.

The calibration of the model had the goal to accurately represent runout distances, jump heights and velocities. Model input parameters derived from this calibration process were then applied to separate sites with broadly similar characteristics as a means of validating the model. A pseudo-forward analysis showed that these input parameters resulted in realistic estimates of the rock fall dynamics and/or runout. There has not been an attempt to directly compare the PIERRE 2 model results to those from other rock fall modelling software at this time.

The model has also been developed with the objective of providing design input values that are safe, but not overly conservative. Hypothetical design calculations compared to observed jump heights and kinetic energies show that the results are appropriate for design purposes. The model presented here is well-suited for application to quantitative hazard assessment.

ACKNOWLEDGEMENTS

The authors would like to thank Prof. Alexander Preh for his assistance with developing the hyperbolic restitution factors and his work with the Austrian quarry study. Data was generously provided by the IRSTEA Institute in Grenoble, France. We would also like to thank Dr. Valentin Gischig for his work with developing the 3D version of this model.

REFERENCES

Abbruzzese, J. M. and Labiouse, V. 2014. New Cadanav methodology for quantitative rock fall hazard assessment and zoning at the local scale, *Landslides*, 11: 551-564.

Bourrier, F. and Hungr, O. 2012. *Rockfall dynamics: A critical review of collision and rebound models, In Rockfall Engineering*, e*dited by* S. Lambert and F. Nicot. John Wiley & Sons, Inc., Hoboken, NJ, USA.

Dorren, L.K.A., Berger, F., Le Hir, C., Mermin, E., Tardif, P. 2005. Mechanisms, effects and management implications of rockfall in forests, *Forest Ecology and Management*, 215(1–3): 183–195

Duncan, J. M. 2000. Factor of safety and reliability in geotechnical engineering, *Journal of Geotechnical and Geoenvironmental Engineering*, 126: 307-316.

Forrestal, M. J. and Luk, V. K. 1992. Penetration into soil targets, *International Journal of Impact Engineering*, 12(3): 427-444.

Gischig, V., Hungr, O., Mitchell, A., Bourrier, F. 2015. Pierre3D – a 3D stochastic rock fall simulator based on random ground roughness and hyperbolic restitution coefficients. *Canadian Geotechnical Journal*, in press.

Goldsmith, W. 1960. *Impact: The theory and physical behaviour of colliding solids*. Edward Arnold (Publishers) Ltd, London.

Mitchell, A. D. 2015. Computer modelling of rock fall: Improvement and calibration of the PIERRE 2 stochastic rock fall simulation program. M. A. Sc. Thesis, University of British Columbia, Vancouver, BC.

Peila, D. and Ronco, C. 2009. Technical note: Design of rockfall net fences and the new ETAG 027 European guideline, *Natural Hazards and Earth System Sciences*, 9: 1291-1298.

Pfeiffer, T., and Bowen, T. 1989. Computer simulation of rockfalls, *Bulletin of the Association of Engineering Geologists*, 26(1): 135–146.

Pichler, B., Hellmich, C., Mang, H. A. 2005. Impact of rocks onto gravel, design and evaluation of experiments, *International Journal of Impact Engineering*, 31: 559-578.

Preh, A., Mitchell, A., Hungr, O., Kolenprat, B. 2015. Stochastic analysis of rock fall dynamics on quarry slopes, *International Journal of Rock Mechanics and Mining Sciences*, in review.

Turner, A. K., and Duffy, J. D. 2012. Evaluation of rockfall mechanics, *In Rockfall: characterization and control, edited by* A. K. Turner, and R. L. Schuster. Transportation Research Board, National Academy of Sciences, Washington DC.

Ushiro, T., Kusumoto, M., Shinohara, S., Kinoshita, K. 2006. An experimental study related to rock fall movement mechanism (*In Japanese)*, *Journal of Japanese Society of Civil Engineers*, 62(2): 377-386.

Volkwein, A., Schellenberg, K., Labiouse, V., Agliardi, F., Berger, F., Bourrier, F., Dorren, L. K. A., Gerber, W., Jaboyedoff, M. 2011. Rockfall characteriszation and structural protection – a review, *Natural Hazards and Earth Systems Sciences*, 11: 2617-2651.

Wyllie, D.C. 2014. Calibration of rock fall modeling parameters, *International Journal of Rock Mechanics and Mining Sciences*, 67: 170-180.